Volume : 2 | Issue : 12 | December 2013 • ISSN No 2277 - 8179

Research Paper

Improvement in IMRT dose calculation with penumbral corrected AAA algorithm using film dosimetry

Medical Science

KEYWORDS: Film dosimetry; Penumbra; Analytical Anisotropic Algorithm; IMRT

Arvind K. Shukla	Research Scholar, Punjab Technical University (PTU), Jalandhar-144601 (India)
Sanjeev Kumar	Department of Physics, G.G.D.S.D. College, Sector-32 C, Chandigarh 160030 (India).
I.S. Sandhu	Department of Applied Sciences, Chitkara University, Rajpura 140 401(India).
Arun S. Oinam	Department of Radiotherapy, Post Graduate Institute of Medical Education and Research, Chandigarh-160 012 (India).
Gaurav Trivedi	Department of Radiotherapy, Post Graduate Institute of Medical Education and Research, Chandigarh-160 012 (India).

ABSTRACT

Background. The accuracy of dose calculation by any treatment planning system for linear accelerator based intensity modulated radiation therapy (IMRT) has always been a concern in radiotherapy. The commissioning data taken with standard ion chamber broaden the measured beam penumbrae leads to inaccuracy in IMRT planning. To achieve good results, a radiation detector with small volume and high spatial resolution has to be used for penumbra measurements.

Materials and methods. The penumbra measurements at several depth and field sizes were performed in water phantom and solid water phantom with 0.13cc ionization chamber and radiographic films, respectively. The IMRT dose calculations were done with an anisotropic analytical algorithm (AAA) using commissioning data taken with and without the use of film dosimetry. The accuracy of these calculations was investigated from the two highly modulated test patterns constructed using Eclipse treatment planning system.

Results. The widths of 80%-20% penumbrae showed increasing trend with increase in the depth of phantom and nearly independent from field sizes except for smaller fields. The highly modulated test patterns exhibit good agreement between the AAA-Film model calculated and measured dose at both 10 cm and 20 cm depths. However, AAA-IC model calculated are significantly lower than measurements at local maxima and higher than measurements at local minima.

Conclusions. These results clearly affirms that accurately measuring of beam penumbrae improves the accuracy of dose distributions calculated by treatment planning system and it is important when commissioning the IMRT.

Introduction

Intensity-modulated radiation therapy (IMRT) is an advanced conformal radiotherapy that delivers highly precise radiation doses to the irregular shaped malignant tumors using computer-controlled linear accelerators (1). The dose distributions in IMRT are systematically synthesized by superimposing several nominal uniform beam segments of different shape. The superposition radiation beams can be done in static or dynamic way. In IMRT planning, calculated and delivered dose depends on multileaf collimators (MLCs) leaf characteristics, i.e., tongue and groove design (2,3) leaf end curvature and radiation leakage through MLC (4,5). An inaccurate calculation of the penumbra can result in cold or hot spots between two adjacent beam segments.

Sharp beam edges with small aperture margin have clear advantages for sparing of normal tissue (6) and the dose gradient is a limiting factor to minimizing radiation exposure to nearby critical structures (7, 8).

A key issue in commissioning of any treatment planning system is to confirm the accuracy of calculated dose with actual dose delivered to the patient. One area that is fundamental to the commissioning process is ensuring the accuracy of the standard data taken with linear accelerator and used as input to the beam models in the IMRT treatment planning system (9-12). Most of beam models commonly used standard data taken with large volume ionization chambers (0.1– 0.2 cm3) at the time of commissioning. The large size standard detectors exhibit penumbra broadening due to high dose gradients and lack of charge particle equilibrium. As a result detector read-out value may deviate from the actual absorbed dose in the target volume. The volume effects of detectors were investigated experimentally by the measuring the penumbra widths. A high precision measurement of beam penumbra requires a detector with high sensitivity, high spatial resolution and practically no energy dependence. The dosimetry of small fields have been reported for parallel-plate chambers, TLDs, diamond detectors, plastic scintillators, ionization chambers, MOSFET detectors, Si diodes, radiochromic and radiographic film (13-15).

The high spatial resolution, limited energy dependence, nearly tissue equivalence and dynamic range of radiochromic and radiographic films are particular attractive for dosimetric measurements in penumbral regions (16). Different approaches have been used to test the accuracy of dose calculated by various algorithms in treatment planning system. Eclipse treatment planning system (Varian Medical Systems) employs pencil beam convolution (PBC) and the anisotropic analytic algorithm (AAA) algorithm to calculate the radiation dose.

In the field axis, the results obtained from PBC model agrees well with the measurements. However, this model exhibit large discrepancies in the penumbral region, especially for rectangular and square-wedged fields (17). On the other hand, AAA model based on pre-calculated Monte Carlo simulations (18) and takes into account electron contamination and extra focal radiation (19). Although there has been much discussion of dosimeters for the verification of IMRT fields there has been less attention to dosimetry in the basic data collection stage of IMRT commissioning (9, 11). The accuracy of PBC model in IMRT has been reported in literature (20).

The aim of present work is to investigate the ability of radiographic film to measure radiation doses in the penumbral region and accuracy of IMRT field calculated by anisotropic analytical algorithm

Volume : 2 | Issue : 12 | December 2013• ISSN No 2277 - 8179

(AAA) model used in the Eclipse Treatment planning system. The beam profiles in penumbral regions were adjusted using data taken with radiographic film. The IMRT calculation using the high-resolution film-corrected data gave good agreement with measurements.

Materials and methods

The present measurements were carried on a Clinac DBX linear accelerator (Varian Medical Systems) equipped with millennium 80-leaf MLCs for 6 MV photon beams in a water phantom (blue phantom2, 48 cm 48 cm 41cm) at various field sizes and depths. Commissioning data used in treatment planning system was taken at different depth with water proof ionization chamber (CC13, IBA dosimetry, Germany) using Omni pro accept V7 (IBA Dosimetry GmBH, Germany) software. Film measurements with extended dose rate (EDR2, Kodak, Radiation Products Design, Inc.) were also performed on a DBX linear accelerator for 6 MV photon beam in 30 30 30 cm3 solid water slab phantom SP34 (Gammex Inc. Middleton, WI) at 100 cm source to surface distance (SSD). All the films were placed perpendicular to the central axis, as shown in Figure 1 and irradiated at room temperature (22° C + 2° C).

Fig.1. Experimental setup of film irradiation for penumbra measurement in solid water phantom.

The sensitometric curve of film optical density and radiation dose was generated from single extended dose rate (EDR 2) film exposed with nine 6×6 cm2 fields with radiation doses raging from 10 to 362 cGy. Irradiated films were analyzed with VIDAR film scanner (VXR-16) and Omni pro IMRT software (IBA dosimetry, Germany) to obtain the value of optical densities at various region.

The penumbra measurements were performed in cross line with ionization chamber and film dosimetry in water phantom and solid water phantom, respectively. The films were placed at 100 cm source-to-surface distance at the various depths. The depths were kept as 1.4, 5, 10, 20 and 30 cm. For each depth, separate films were exposed for square fields of 4, 6, 10, 20, 30 and 40 cm2 with 100 cGy dose. In IMRT measurements two sets of 6 MV data were taken with ionization chamber and radiographic films. The first set of data included depth dose and lateral profile data gathered in a water phantom, using a water proof ionization chamber, and referred as AAA-IC. The second set of input data used in AAA commissioning was very similar to the first, with the exception that the penumbral regions of the open field profiles were adjusted to coincide with the penumbrae measured by radiographic film. The second set of corrected data is referred AAA-Film.

Results

The cross beam profiles and the penumbral portion of the off axis data for the 10 x 10 cm2 open field measured with ion chamber and radiographic film at 10 cm depth are shown in Figure 2 (a) (b), respectively.

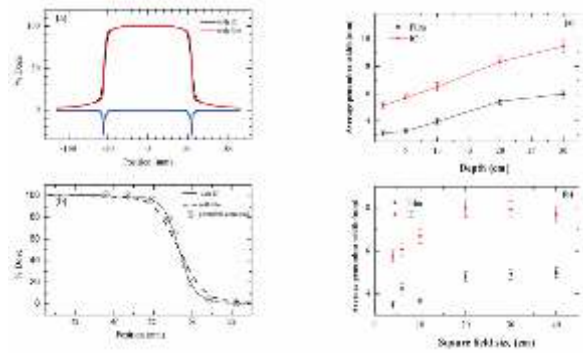

Fig.2. (a) Cross profiles measured with ion chamber (IC) and radiographic film for 10 ×10 cm2 field size at 10 cm depth. Blue and cyan color lines represent the difference between measured ion chamber and film corrected profiles and (b) the penumbral region of a 10×10 cm2 open field at 10 cm depth measured using IC and radiographic film. The IC chamber data were adjusted using film data to represent the shape of real penumbra.

Fig.3. Variation of average penumbra broadening with (a) several measuring depths and (b) various open field size length.

Figure 2 clearly demonstrates that measured beam profiles are in good agreement in the square open field and exhibit large deviation in the penumbra region. The measured penumbra widths at several depths and field sizes in water phantom for 6 MV photon beam are listed in Table 1. The sharpest 80%-20% penumbra of 2.91 mm was obtained at a depth of 1.4 cm. It is clear from Table 1that the width of penumbra calculated using film dosimetry and ionization chamber measurements showed increasing trend with increase the depth of the phantom. However, the dependency of the penumbra width on field sizes only predominant for smaller fields and nearly independent for larger field sizes. The variations of average penumbra with depth and field size are also shown in Figure 3a and Figure 3b, respectively.

Table 1: 80%-20% penumbra width (mm) calculated for various beam configurations using IC and radiographic film.

Depth (cm)	Radiation detectors	Field sizes					
		4 X4 cm²	*6X 6 cm²*	*10X10 cm²*	*2020 cm²*	*30X30 cm²*	*40X40 cm²*
1.4	*Film*	*2.91*	*3.24*	*2.98*	*3.24*	*3.14*	*3.10*
	IC	*5.04*	*5.20*	*4.53*	*5.23*	*5.40*	*5.35*
5	*Film*	*3.22*	*3.29*	*3.26*	*3.32*	*3.57*	*3.33*
	IC	*5.04*	*5.20*	*5.80*	*6.04*	*6.07*	*6.00*
10	*Film*	*3.39*	*4.06*	*3.95*	*4.50*	*5.77*	*3.11*
	IC	*5.60*	*6.00*	*6.47*	*7.20*	*7.776*	*5.98*
20	*Film*	*3.92*	*4.27*	*4.28*	*5.18*	*5.54*	*7.50*
	IC	*6.34*	*6.78*	*7.70*	*9.40*	*10.00*	*9.80*
30	*Film*	*3.95*	*4.79*	*4.98*	*6.68*	*6.60*	*7.90*
	IC	*6.77*	*7.20*	*8.96*	*11.02*	*10.04*	*11.40*

The dose calculation AAA algorithm used in eclipse treatment planning system was originally developed by Ulmer et al. (21-23). The use of exponential functions reduces boundary artifacts due to tissue inhomogeneous factor and enables faster dose distribution calculations. Inhomogeneities are taken into account by lateral density scaling of the photon scatter kernel, depth dependent

correction factors, and also a "history correction convolution," introduced in the depth direction to model changes of electronic fluence conditions at interfaces. The initial photon spectrum just below the target is taken from the Eclipse database and was pre calculated by Monte Carlo simulation using (24). The beam is divided into fanlines (beamlets) and the convolutions are performed, for each beamlet comprised in the clinical beam, using kernels and an intensity function. The final dose distribution is obtained by a superposition of the dose contribution of each individual beamlet. The shape of each kernel depends upon off-axis ratio and can be constructed using the slopes of the open beam profile through the penumbra region. For the AAA-IC and AAA-Film algorithms, beam kernels were calculated by the Eclipse planning system from the two data sets. A separate kernel was calculated for each algorithm corresponding to the water depths of 1.4, 5, 10, 20, and 30 cm. It is clearly seen from Figure 4 that the effect of the steeper slopes of the film-corrected penumbrae in the narrowing of the beam kernels representing the AAA-Film algorithm relative to the beam kernels of the AAA-IC algorithm.

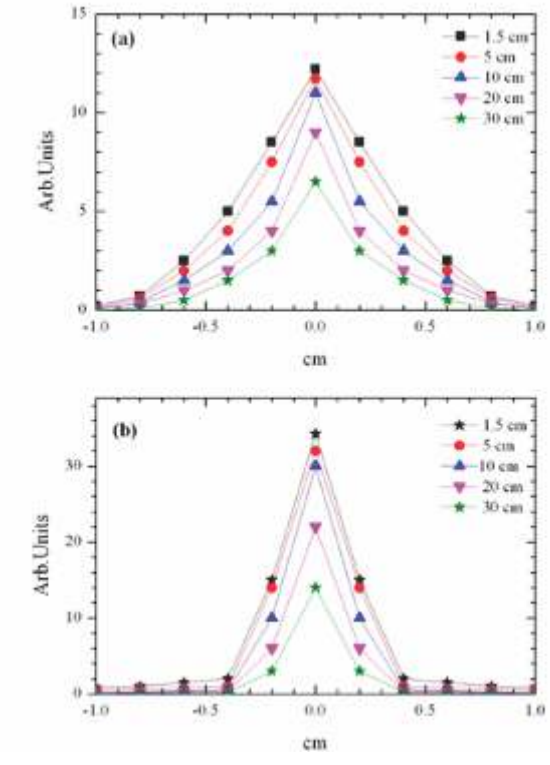

Fig.4. Pencil beam kernels calculated at different depths using (a) IC and (b) Film-corrected data sets.

Two test patterns with a series of peaks and valleys were created using static and dynamic intensity modulation with Eclipse treatment planning system separately. The measurement depths for each plan were kept at 10 cm and 20 cm, respectively. In case of static test pattern (Figure 5a) the calculated individual dose maxima for all six peaks were an average of 10% lower than the measured maxima, and the calculated minima for all five valleys were on average about 16 % higher than measurements. Similar deviation has been noticed at 20 cm depth (Figure 5c).

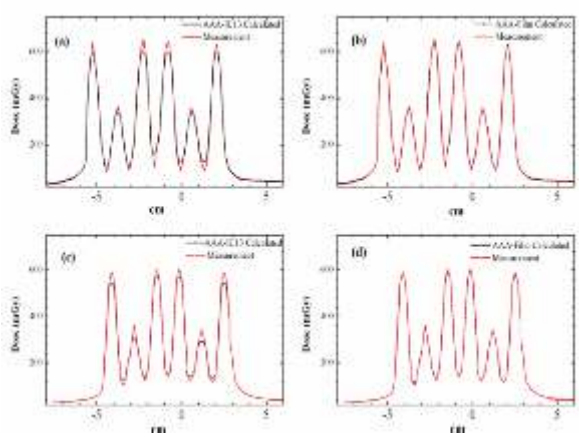

Fig.5. Comparison of AAA-IC and AAA-Film based static field IMRT test patterns with measured dose in water equivalent phantom at 10 cm [(a) and (b)] and 20 cm [(c) and (d)] depths.

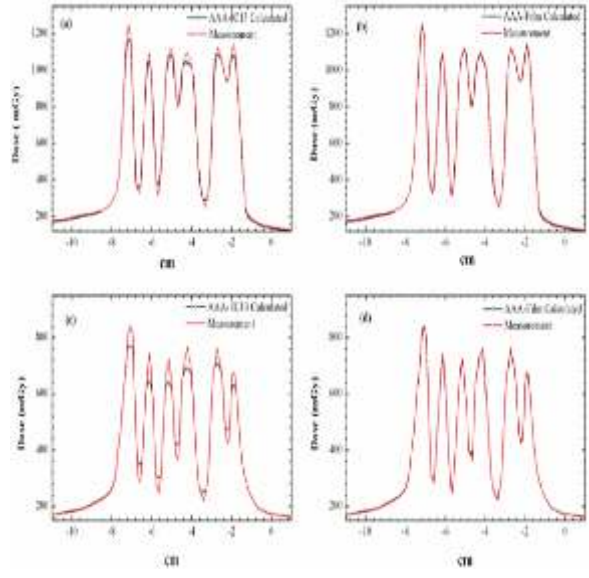

Fig.6. Comparison of AAA-IC and AAA-Film based dynamic field IMRT test patterns with measured dose in water equivalent phantom at 10 cm [(a) and (b)] and 20 cm [(c) and (d)] depths.

The comparison between measurements and calculations for the AAA-Film model is shown in (Figure 5b and Figure 5d). In this case the agreement between the AAA calculations and the measured dose is much better and within 3 % for maxima and minima than for the uncorrected AAA model, at both 10 and 20 cm depths. Likewise, in case of dynamic test pattern (Figure 6a and 6c) the calculated individual dose maxima for all six peaks were an average of 9 % lower than the measured maxima, and the calculated minima for all five valleys were on average about 13 % higher than measurements. The comparison between measurements and calculations for the AAA-Film model are also shown in Figure 6b at 10 cm depth and Figure 6d at 20 cm depth. Like static model, the dynamic IMRT based on AAA-Film model show no significant differences between calculations and measurements.

Discussion

This study shows that volume effect of ion chamber underestimated the true dose inside the fields while overestimating it outside the field. The measurements performed with ionization chamber exhibit less sharp penumbra as compare to the data taken with high spatial resolution radiographic film in high dose gradient region. Hence, the width penumbra mainly

depends upon measurement method rather than the algorithm used for dose calculation in treatment planning system. Because of the high spatial resolution of film and of the scanner, the penumbra measured with film is close to the real penumbra of the beam. It has been well established that penumbra width measured with radiographic films are very close to those measured by other high-resolution detectors such as silicon detectors, TLD and diamond detectors (25,11,16). The present results on penumbra measurements are in well agreement with the earlier reported results by Huq et al. (26), Das et al. (2) and Galvin et al. (27) for the various linear accelerators used in radiotherapy. The differences between measured and calculated IMRT fields depend upon beam kernels evaluated by AAA model. As a result, the standard data measured with ion chamber led to the inaccurate calculation of dose kernels than one measured with high resolution film.

Conclusions

It is clear from present measurements that the accuracy of IMRT dose calculations would be significantly depends upon the resolution of the detector used in beam data collection. Main source of discrepancies in measured and calculated IMRT data can be attributed to detector volume effect in the commissioning data. The detector broadened penumbrae led to the inaccurate calculation of dose kernels in the AAA model. The error arises from kernels derived from inaccurate penumbra measurements could lead to inaccurate dose volume histogram (DVH) calculations. Hence, the final doses calculated by treatment planning system will contain such errors if it used the commissioning data taken with large volume ionization chambers. The results presented here affirm the importance of choosing an appropriate detector when gathering off-axis data for IMRT commissioning.

Acknowledgement

One of us author (AKS) would also like to thank the Punjab Technical University, Jalandhar for facilitating research work.

Conflict of interest: No conflict of interest.

REFERENCE

1. Sanghani M, Mignano J. Intensity Modulated Radiation Therapy: A Review of Current Practice and Future Directions. Technol Cancer Res Treat 2006; 5: 447-50|2. Das IJ, Desobery GE, McNeeley SW, Cheng EC, Schultheiss TS. Beam characteristics of a retrofitted double focused multileaf collimator. Med Phys 1998; 25: 1776-84.|3. Van Santvoort JPC, Heijmen BJM. Dynamic multileaf collimation without 'tongue-and-groove' under dosage affects. Phys Med Biol 1996; 41: 2091-105.|4. Wang X, Spirou S, LoSasso T, Stein J, Chui CS, Mohan R. Dosimetric verification of intensity-modulated fields. Med Phys 1996; 23: 317-27.|5. LoSasso T, Chui CS, Ling CC. Physical and dosimetric aspects of a multileaf collimation system used in the dynamic mode for implementing intensity modulated radiotherapy. Med Phys 1998; 25: 1919-27.|6. Sharpe MB, Jaffray DA, Battista JJ, Munro P. Extra focal radiation: a unified approach to the prediction of beam penumbra and output factors for megavoltage x-ray beams. Med Phys 1995; 22: 2065-74.|7. Bova FJ, Buatti JM, Friedman WA, Mendenhall WM, Yang CC, Liu C. The University of Florida frameless high-precision stereotactic radiotherapy system. Int J Radiat Oncol Biol Phys 1997; 38: 875-82.|8. Schulte RW, Fargo RA, Meinass HJ, Slater JD, Slater JM. Analysis of head motion prior to and during proton beam therapy. Int J Radiat Oncol Biol Phys 2000; 47: 1105-10.|9. Van Esch A, Bohsung J, Sorvari P, Tenhunen M, Paiusco M, Iori M, Engstrom P, Nystrom H, Huyskens DP. Acceptance tests and quality control (QC) procedures for the clinical implementation of intensity modulated radiotherapy (IMRT) using inverse planning and the sliding window technique: Experience from five radiotherapy departments. Radiother Oncol 2002; 65: 53-70.|10. Ezzell GA, Galvin JM, Low D, Palta JR, Rosen I, Sharpe MB, Xia P, Xiao Y, Xing L, Yu CX. Guidance document on delivery, treatment planning, and clinical implementation of IMRT: Report of the IMRT subcommittee of the AAPM radiation therapy committee. Med Phys 2003; 30: 2089-115.|11. Laub WU, Wong T. The volume effect of detectors in the dosimetry of small fields used in IMRT. Med Phys 2003; 30: 341-7.|12. Otto K, Alkins R, Clark BG. Improved IMRT dose calculations using pencil beam kernels derived from high resolution film dosimetry, in Proceedings of the 49th Annual Scientific Meeting, Canadian Organization of Medical Physicists 2003; pp. 87-9.|13. Francescon P, Cora S, Cavedon C, Scalchi P, Reccanello S, Colombo F. Use of a new type of radiochromic film, a new parallel-plate micro-chamber, MOSFETs, and TLD 800 microcubes in the dosimetry of small beams. Med Phys 1998; 25: 503-11.|14. Serago CF, Houdek PV, Hartmann GH, Saini DS, Serago ME, Kaydee A. Tissue maximum ratios (and other parameters) of small circular 4, 6, 10, 15 and 24 MV x-ray beams for radiosurgery. Phys Med Biol 1992; 37: 1943-56.|15. Heydarian M, Hoban PW, Beddoe AH. A comparison of dosimetry techniques in stereotactic radiosurgery. Phys Med Biol 1996; 41: 93-110.|16.Butson MJ, Yu PKN, Cheung T. Rounded end multi-leaf penumbral measurements with radiochromic film. Phys Med Bio 2003; 48: N247-N252.|17. Storchi P, Woudstra E. Calculation of the absorbed dose distribution due to irregularly shaped photon beams using pencil beam kernels derived from basic beam data. Phys Med Biol 1996; 41: 637-56.|18.Sievinen J, Ulmer W, Kaissl W. AAA photon dose calculation model in Eclipse. Palo Alto (CA): Varian Medical Systems 2005; [RAD #7170B].|19.Varian Medical Systems. The reference guide for Eclipse algorithms. Palo Alto (CA): Varian Medical Systems. 2005; [P/N B401653R01M].|20.Arnfield MR, Otto K, Aroumougame VR, Alkins RD. The use of film dosimetry of the penumbra region to improve the accuracy of intensity modulated radiotherapy. Med Phys 2005; 32: 12-8.|21.Ulmer W, Harder D. A triple Gaussian pencil beam model for photon beam treatment planning. Z Med Phys 1995; 5: 25-30.|22.Ulmer W, Kaissl W. The inverse problem of a Gaussian convolution and its application to the finite size of the measurement chambers/detectors in photon and proton dosimetry. Phys Med Biol 2003; 48: 707-27.|23.Ulmer W, Pyyry J, Kaissl W. A 3D photon superposition/convolution algorithm and its foundation on results of Monte Carlo calculations. Phys Med Biol 2005; 50:1767-90.|24.Rogers DW, Faddegon BA, Ding GX, Ma CM, We J, Mackie TR. BEAM: a Monte Carlo code to simulate radiotherapy treatments units. Med Phys 1995; 22: 503-24.|25.Metcalfe P, Kron T, Elliot A, Wong T, Hoban P. Dosimetry of 6-MV x-ray beam penumbra. Med Phys 1993; 20: 1439-45.|26.Huq MS, Yu Y, Chen ZP, Suntharalingam N. Dosimetric characteristics of a commercial multileaf collimator. Med Phys 1995; 22: 241-7.|27.Galvin JM, Smith AR, Lally B. Characterization of a multi leaf collimator system. Int J Radiat Oncol Bio Phys 1993; 25: 181-92.